AFOSR-TR- 82-0550

(5)

FINAL TECHNICAL REPORT

submitted to the

Air Force Office of Scientific Research

by the

Geophysics Laboratory
University of Southern California

Contractor:	University of Southern California
Date of Contract:	July 2, 1976 to April 30, 1982
Amount of Contract:	$214,002
Contract Number:	F49620-76-C-0010
Principal Investigator:	Ta-liang Teng Professor of Geophysics (213) 743-6124
Program Managr:	Bill Best
Title:	CRUSTAL AND UPPER MANTLE VELOCITY AND Q OF MAINLAND CHINA
Sponsored by:	Advanced Research Projects Agency (DOD) ARPA Order No. 3291
Date of Report:	May, 1982

U.S.C. GEOPHYSICS LABORATORY TECHNICAL REPORT #82-8

~~UNCLASSIFIED~~
SECURITY CLASSIFICATION OF THIS PAGE (When Data Entered)

REPORT DOCUMENTATION PAGE		READ INSTRUCTIONS BEFORE COMPLETING FORM
1. REPORT NUMBER AFOSR-TR- 82-0550	2. GOVT ACCESSION NO. AD-A117030	3. RECIPIENT'S CATALOG NUMBER
4. TITLE (and Subtitle) CRUSTAL AND UPPER MANTLE VELOCITY AND Q OF MAINLAND CHINA		5. TYPE OF REPORT & PERIOD COVERED Final 02 Jul 76 to 30 Apr 82 6. PERFORMING ORG. REPORT NUMBER
7. AUTHOR(s) Ta-liang Teng		8. CONTRACT OR GRANT NUMBER(s) F49620-76-C-0010
9. PERFORMING ORGANIZATION NAME AND ADDRESS University of Southern California Department of Geological Sciences Los Angeles, California 90089		10. PROGRAM ELEMENT, PROJECT, TASK AREA & WORK UNIT NUMBERS 61102F 3291/40
11. CONTROLLING OFFICE NAME AND ADDRESS AFOSR/NP Bolling AFB, Bldg. #410 Wash DC 20332		12. REPORT DATE May, 1982 13. NUMBER OF PAGES 28
14. MONITORING AGENCY NAME & ADDRESS(if different from Controlling Office)		15. SECURITY CLASS. (of this report) Unclassified 15a. DECLASSIFICATION/DOWNGRADING SCHEDULE

16. DISTRIBUTION STATEMENT (of this Report)

Approved for public release; distribution unlimited

17. DISTRIBUTION STATEMENT (of the abstract entered in Block 20, if different from Report)

18. SUPPLEMENTARY NOTES

DTIC COPY INSPECTED 2

Accession For	
NTIS GRA&I	☒
DTIC TAB	☐
Unannounced	☐
Justification	
By	
Distribution/	
Availability Codes	
Dist	Avail and/or Special
A	

19. KEY WORDS (Continue on reverse side if necessary and identify by block number)

20. ABSTRACT (Continue on reverse side if necessary and identify by block number)

The temporal resolution and accuracy of FTAN (frequency-time analysis) as applied to surface wave dispersion analysis are examined for a period range from 10 to 200 seconds. The constant relative bandwidth filter (~~Dziewonski et al.,1969~~), optimum bandwidth filter (~~Inston et al.,1971~~) and display-equalized filter (~~Nyman and Landisman, 1977~~) are carefully examined with respect to their adequacy of application over a broad period range. Among these Gaussian filters, the optimum bandwidth filter gives a better performance for relatively short-period (less than 50 seconds) dispersion measurement. To measure surface-wave dispersion for a broad

DD FORM 1 JAN 73 1473

UNCLASSIFIED
SECURITY CLASSIFICATION OF THIS PAGE (When Data Entered)

20. period range, a 'matched-filter FTAN' technique is introduced by modifying the 'residual dispersion measurement' technique (Dziewonski et al., 1972). A detailed numerical analysis is made on this new technique, the result demonstrates a significant improvement on both the resolution and the accuracy of surface wave dispersion data extraction over a broad period range up to at least 200 seconds.

USC GEOPHYSICS LABORATORY TECHNICAL REPORT #82-8

Department of Geological Sciences
University of Southern California
Los Angeles, California 90089

Final Technical Report for AFOSR Contract #F49620-76-C-0010

ARPA Order:	3291
Program Code:	TF10-7F10
Name of Contractor:	University of Southern California
Effective Date of Contract:	July 2, 1976
Contract Expiration Date:	April 30, 1982
Amount of Contract:	$214,002.00
Contract Number:	F49620-76-C-0010
Principal Investigator:	Ta-liang Teng Professor of Geophysics (213) 741-6124
Program Manager:	William Best (202) 766-4908
Title of Work:	CRUSTAL AND UPPER MANTLE VELOCITY AND Q STRUCTURES OF MAINLAND CHINA

Sponsored by
Advanced Research Projects Agency (DOD)
ARPA Order No. 3291
Monitored by AFOSR Under Contract #F49620-76-C-0010

May, 1982

AN ERROR ANALYSIS OF FTAN

Chi-Chin Feng and Ta-Liang Teng

Department of Geological Sciences
University of Southern California
Los Angeles, California 90007

submitted to Bulletin of the
Seismological Society of America

February 1982

ABSTRACT

The temporal resolution and accuracy of FTAN (frequency-time analysis) as applied to surface wave dispersion analysis are examined for a period range from 10 to 200 seconds. The constant relative bandwidth filter (Dziewonski et al., 1969), optimum bandwidth filter (Inston et al., 1971) and display-equalized filter (Nyman and Landisman, 1977) are carefully examined with respect to their adequacy of application over a broad period range. Among these Gaussian filters, the optimum bandwidth filter gives a better performance for relatively short-period (less than 50 seconds) dispersion measurement. To measure surface-wave dispersion for a broad period range, a 'matched-filter FTAN' technique is introduced by modifying the 'residual dispersion measurement' technique (Dziewonski et al., 1972). A detailed numerical analysis is made on this new technique, the result demonstrates a significant improvement on both the resolution and the accuracy of surface wave dispersion data extraction over a broad period range up to at least 200 seconds.

INTRODUCTION

Surface-wave dispersion measurement determines the phase angle, amplitude and group arrival time of surface waves as a function of period. These data are important for studies of the crust-upper mantle structure, the source mechanism of earthquakes and the anelastic properties of the earth.

A peak-and-trough method was employed in most of the early surface-wave studies (e.g., Ewing and Press, 1952; 1954). From the arrival times of different phases (peaks, zeros and troughs), the phase angle, amplitude and group arrival time of a dispersed signal can be determined graphically as a function of period. Obviously, this technique is only feasible for analyses of well-dispersed signals.

Satô (1955) suggested calculation of the dispersion data directly from the Fourier transform of the signal. This method has the advantage of being applicable to the less dispersed, short wave trains where the peak-and-trough method is not satisfactory. However, the application of this method is limited to a frequency range where the signal-noise ratio is high.

In order to extend the resolution of dispersion measurement to a broader period range, it is natural to consider the use of a filtering technique to enhance the signal-noise ratio. Landisman et al. (1969) introduced the 'moving window analysis' which estimates a complex quantity $C(\omega,t)$ from the convolution of the signal $f(t)$ with a filter $g_\omega(t)$, giving

$$C(\omega,t) = \int_{-\infty}^{\infty} f(\tau) g_\omega(t-\tau) d\tau \qquad (1)$$

where

$$g_\omega(t) = h_\omega(t)\exp(i\omega t)$$

and h_ω is a symmetric window function.

A different method, the 'multiple filter technique', was introduced by Dziewonski et al. (1969) which determines C by an inverse Fourier transformation of the band-passed spectrum. In this case we have

$$C(\omega,t) = \frac{1}{2\pi} \int_{-\infty}^{\infty} H_\omega(\Omega-\omega)F(\Omega)\exp(i\Omega t)d\Omega \qquad (2)$$

where

$$F(\omega) = \int_{-\infty}^{\infty} f(t)\exp(-i\omega t)dt$$

is the Fourier transform of the signal f and H_ω is a symmetric band-pass filter.

If h_ω and H_ω are a Fourier transform pair,

$$H_\omega(\Omega) = \int_{-\infty}^{\infty} h_\omega(t)\exp(-i\Omega t)dt,$$

$$h_\omega(t) = \frac{1}{2\pi}\int_{-\infty}^{\infty} H_\omega(\Omega)\exp(i\Omega t)d\Omega$$

expressions (1) and (2) are equivalent. The equivalence of these two methods indicates that regardless of our choice of filter in the time or frequency domain, the actual filtering effect is the same. These two different but equivalent methods, the 'moving window analysis' and the 'multiple filter technique', are now generally referred to as frequency-time analysis (FTAN).

FTAN determines the group arrival time t_g at frequency ω as the time when the absolute value of $C(\omega,t)$ in (1) or (2) achieves its maximum value. The inferred phase angle and amplitude at frequency ω are then determined as the phase and amplitude of the complex quantity $C(\omega,t_g)$.

A Gaussian filter is generally used in FTAN. If the Fourier transform pair h_ω and H_ω in (1) and (2) are Gaussian filters, then they can be written as

$$H_\omega(\Omega) = \exp(-\gamma\Omega^2)$$

$$h_\omega(t) = (4\pi\gamma)^{-1/2}\exp(-t^2/4\gamma)$$

where γ is a constant which controls the bandwidth of the Gaussian filter. In frequency and time domains, the bandwidths are, respectively

$$\delta H = \gamma^{-1/2}$$

$$\delta h = 2\gamma^{1/2}$$

Instead of γ, however, we shall use the Gaussian parameter α defined by Dziewonski et al. (1969) for all the following discussions. The parameter α controls the relative bandwidth of a Gaussian filter, and is related to γ by

$$\alpha = \gamma\omega^2.$$

It is important to understand the filtering effects due to different α values, because α is the only parameter which is adjustable in the application of FTAN. We shall use the 'averaging region' (Nyman and Landisman, 1977) of a filter to demonstrate its filtering effect. The shape of 'averaging region', which is an ellipse with radii δH and δh in the frequency and time axes, gives very clear insight into the filtering effect. For a given period, the quotient $\delta h/\delta H$ is proportional to α. For a constant α, this quotient is proportional to the square of period. Figure 1 shows the 'averaging region' of several α values in the velocity-log period plane at an epicentral distance of 9453.61 km. A seismogram recorded at such a distance will be used for various numerical tests. Since we are using in Figure 1 the velocity-log period domain instead of time-frequency domain, the time is mapped to the velocity axis based on the epicentral distance. The choice of the above epicentral distance only makes the contents of Figure 1 consistent with the results in late figures without losing the generality of the findings.

Based on different considerations, three representative Gaussian filters have been proposed for FTAN.

A constant α value for all periods was used in the original multiple filter technique (Dziewonski, et al., 1969), which has become the most commonly used

filter for FTAN technique. We shall refer to this filter as the 'constant relative bandwidth filter' (CRBF).

The display-equalized filter (DEF) by Nyman and Landisman (1977) is a filter which averages the signal in a more natural way. The 'averaging region' of DEF is approximately a circle, although varying in size, throughout the frequency-time domain.

The most complicated filter is the optimum bandwidth filter (OBF) by Inston et al. (1971) and Cara (1973) which was designed to maximize the temporal resolution in the application of the FTAN. To construct an OBF requires the approximate dispersion properties of the signal that is to be analyzed. They are obtained either from the literature or determined by any simpler technique much as FTAN with CRBF.

NUMERICAL EXPERIMENTS

The objective of FTAN is to enhance the resolution of dispersion measurement by smoothing the dispersion data. However, systematic errors of FTAN are generated by the filtering at periods where the amplitude spectrum or phase spectrum change rapidly. Dziewonski et al. (1972) have shown that if the second- and higher-order terms of Taylor's expansions of the amplitude and phase spectrums could be neglected, then little systematic errors would be introduced.

The seismograms shown in Figure 2 are used to examine the temporal resolution and accuracy of FTAN with different Gaussian filters. The top trace of Figure 2 is the vertical seismogram of a Taiwan earthquake of 1978 December 23, recorded at the SRO (Seismic Research Observatory) station GRFO in Germany. The epicentral distance is 9453.61 kilometers. A typical surface-wave train such as this one propagating across a laterally heterogeneous crust and upper mantle results in a complex dispersive wave form.

The bottom two traces of Figure 2 are synthetic surface-wave trains which will be our calibration standards for various methods discussed later. To construct seismograms A and B, first, we determine their Fourier spectra based on the group-velocity dispersion curves and amplitude spectra shown in Figures 3 and 4. Then, after filtering the Fourier spectra by the SRO instrument response (Peterson et al., 1976; 1980), an inverse Fourier transform is applied to convert the spectra into wave trains. Finally, a quiescent portion of the SRO record, which may be considered as the average noise background, is added to both wave trains. A comparison of the dispersed seismogram with noise is shown in Figure 5. In the period band of interest, the signal is about two orders of magnitude larger than the noise in a typically well recorded large event by an SRO station.

Figure 6 shows the α values as a function of period for the cases of CRBF, DEF and OBF based on the particular observed seismogram shown in Figure 2. Dziewonski et al. (1972) have pointed out that $\alpha \leq 40$ is more commonly used in practice; here we use $\alpha=40$ for CRBF, because larger α value leads to smaller systematic errors.

Equation (2) rather than (1) is used for the filtering computation in these numerical experiments. There are two reasons to perform the computations in the frequency domain. First, a more efficient algorithm is available to calculate Fourier transforms than convolution. Second, it is easier to compensate the instrument response in the frequency domain.

The wave train to be analyzed is first extended to 8192 points. This extension in data length is important for frequency analysis; it reduces the coarseness of the discrete Fourier spectrum at long period. Then, the Fourier spectrum in (2) is obtained for the extended signal by fast Fourier transform and an instrument response compensation is made. Finally, at each of the center frequencies for analysis, the Fourier spectrum is filtered by the Gaussian filter

$H_\omega(\Omega-\omega)$; then an inverse Fourier transform of the band-passed spectrum is made to obtain $C(\omega,t)$.

The most time-consuming part of FTAN is the inverse Fourier transform, because it must be performed for all the selected center frequencies. The method introduced by Seneff (1978), which can greatly reduce the computation time, is employed in our computational process. The method involves a frequency shift such that the center frequency of the band-pass filter is moved to the origin. The effect is to greatly reduce the apparent bandwidth and allow a reduction of the inverse transform size down to a much smaller number of points.

Figures 7, 8 and 9 give the dispersion results of the top trace in Figure 2 using the CRBF, DEF and OBF. In these figures, the solid dots are the maximum amplitudes which correspond to the estimated group velocities. Also shown are two contours of 1 db and 10 db down from the maximum. These analyses demonstrate that using FTAN with CRBF or DEF might lead to poor resolution for certain period ranges.

Then the synthetic seismogram A is analyzed by FTAN to determine the systematic errors in group velocity and amplitude. Because the α values of DEF are either close to those of CRBF at relatively short periods (10-35 seconds) or to OBF at longer periods (35-400 seconds), we only show here the results produced by CRBF and OBF.

Systematic errors in the determination of group velocity and amplitude for CRBF and OBF are plotted against the period in Figures 10 and 11. For CRBF, the maximum error in group velocity determinations reaches about 0.07 km/sec and the estimated amplitude could be as low as 40% of the actual value. We suspect that the significant distortion at relatively short periods is due to poor resolution. The OBF is good for relatively short periods. For long periods, however, a wider

bandwidth is usually required to obtain good resolution and this introduces larger systematic errors. Because the dispersive property of the synthetic seismogram is smoother than that of actual seismograms, the systematic errors shown here are, therefore, smaller than those of the actual case.

Thus we conclude that OBF is a better filter for FTAN than CRBF. It produces reasonably good resolution in group-velocity determinations for a broad period range and small systematic errors for relatively short periods.

MATCHED-FILTER FTAN

As demonstrated in the previous section, we can find a filter (OBF) to optimize the temporal resolution of FTAN but no filter can remove the systematic errors. We must search for other techniques to improve the accuracy of dispersion measurement.

Systematic errors of FTAN are generated by the filtering process at periods where the second and higher terms of Taylor's expansions of the amplitude or phase spectra are large. Therefore, a simple way to reduce systematic errors is to use a larger α value (narrower relative bandwidth). However, a large α may result in losing the temporal resolution and it is not uncommon to lose resolution completely using a very large α value. In dealing with this property of FTAN, Denny and Chin (1976) introduced an extrapolation algorithm to estimate the group arrival time of a dispersed signal. For a given frequency, they determine several inferred values of group arrival time from a set of filters whose bandwidths are appropriately distributed about the optimum bandwidths. Then, the group arrival time is obtained by extrapolation from these data. Not only is this method complicated in computation, but also it has another intrinsic difficulty. We have already seen in Figure 1 that the shape of the 'averaging region' varies from an elongated horizontal to vertical pattern with increasing α value. Thus the group arrival time obtained by extrapolation may not represent

a better solution if the noise is not very weak or random. This is because the data used for extrapolation have been distorted by different noise content in addition to the deviation purely due to the filtering effect.

Another way to reduce systematic errors is to use the technique of match-filtering. The technique of match-filtering measure the residual signal, which is the cross-correlation of the observed seismogram with a theoretical signal whose dispersion approximates the observed dispersion. Because the residual signal is less dispersive compared to the observed seismogram, the determination of dispersion is more precise, with smaller systematic errors. This technique has been applied by Dziewonski et al. (1972) and is known as the 'residual dispersion measurement' (RDM) technique.

We examine RDM using a synthetic seismogram and found that some improvements are required to make it more suitable for surface-wave dispersion measurement. The shortfalls of RDM include: (1) CRBF is used in RDM, and we have seen previously that this filter produces results with poor temporal resolution except for a certain period range where the α value of CRBF is close to that of OBF, and (2) The amplitude spectrum of the theoretical signals used by RDM is a constant, thus the systematic errors due to the rapid changing nature of amplitude with frequency (which usually exists in observed signal at short periods, i.e. 10-50 seconds) cannot be reduced.

To correct these shortfalls we have made progress building on Dziewonski's work, a new technique of dispersion measurement is designed and introduced here.

Figure 12 illustrates our measurement procedure which is identified as the 'matched-filter FTAN' technique (MF-FTAN). We use the spectrum $A_2(\omega)\exp[i\phi_2(\omega)]$ measured by FTAN with OBF as the first iteration spectrum because usually it has been smoothed and does not have large discontinuities. Then the residual spectrum is constructed by taking the ratio of the observed spectrum $A_1(\omega)\exp(i\phi_1(\omega)]$ to the first iteration spectrum. On top of the phase spectram that Dziewonski has

treated. it is important here to include the amplitude spectrum in the formation of the residual spectrum, because the variation of amplitude with frequency is usually rapid at short periods and thus introduces errors to the FTAN process. The residual spectrum is then analyzed by FTAN with DEF to determine the correction terms for the dispersion data. Because the residual spectrum is nearly white, good resolution can be obtained by using DEF. Finally, the dispersion data are obtained by adding the correction terms to first iterations dispersion data. This measurement procedure can be used iteratively to further improve the analysis. However, experience shows that one iteration usually gives sufficiently good results.

This new measurement procedure has been tested using synthetic seismograms A and B. The systematic errors in group velocity have been reduced substantially to less than 0.02 km/sec (Figure 13). The accuracy of amplitude estimation is also greatly improved (Figure 14). The relative errors in amplitude are less than 10% for periods longer than 20 seconds. The largest error occurs at the 15 second period, where the estimated amplitude is about 70% of the actual amplitude. The accuracy of amplitude determination can be further improved by additional iterations. Figure 15 shows the amplitude ratio of the second iteration result. The largest relative error is reduced to less than 20%. These test results suggest that for group-velocity determination, accurate results can be obtained in the first iteration; for amplitude estimation, a second iteration may be required.

CONCLUSION

Based on the results of a numerical experiment, the optimum bandwidth filter is found most suitable for surface-wave dispersion measurement of periods less than 50 seconds. To improve the resolution of dispersion measurement over a broader period range with reduced systematic errors, a 'matched-filter FTAN'

technique is introduced by modifying the 'residual dispersion measurement' technique. For a period range from 10 to 200 seconds, the maximum error in group velocity is less than 0.02 km/sec and the maximum relative error in amplitude is less than 20 percent. For most periods, however, the errors in group velocity and relative errors in amplitude are about 0.01 km/sec and 5 percent, respectively. The 'matched-filter FTAN' has been applied to a study on the crust-upper mantle structures of Eurasia (Feng, 1982). The improved amplitude estimate would certainly be useful in studies on attentuation using surface waves.

ACKNOWLEDGEMENTS

We thank Charles G. Sammis, Kenneth A. Piper and John McRaney for suggested improvements to the manuscript. This research is supported by the Advanced Research Project Agency of the Department of Defense and is monitored by the Air Force Office of Scientific Research under Contract F49620-76-C-0010.

REFERENCES

Cara, M. (1973). Filtering dispersed wavetrains, Geophys. Jour. 33, 65-80.

Denny, M. D. and R. C. Y. Chin (1976). Gaussian filters for determining group velocities, Geophys. Jour. 45, 495-525.

Dziewonski, A., S. Bloch, and M. Landisman (1969). A technique for the analysis of transient seismic signals, Bull. Seism. Soc. Am. 59, 427-444.

Dziewonski, A., J. Mills, and S. Block (1972). Residual dispersion measurement - a new method of surface-wave analysis, Bull. Seism. Soc. Am. 62, 129-139.

Ewing, M., and F. Press (1952). Crustal structure and surface-wave dispersion, Part II, Solomon Islands earthquake of 29 July 1950, Bull. Seism. Soc. Am. 42, 315-325.

Ewing, M. and F. Press (1954). An investigation of mantle Rayleigh waves, Bull. Seism. Soc. Am. 44, 127-147.

Feng, C. C. (1980). A surface wave study of crustal and upper mantle structures of Eurasia, Ph.D. dissertation, University of Southern California, 293 pp.

Inston, H. H., P. D. Marshall, and C. Blame (1971). Optimization of filter bandwidth in spectral analysis of wavetrains, Geophys. Jour. 23, 243-250.

Landisman, M., A. Dziewonski, and Y. Sato (1969). Recent improvements in the analysis of surface wave observations, Geophys. Jour. 17, 369-403.

Nyman, D. C., and M. Landisman (1977). The display equalized filter for frequency-time analysis, Bull. Seism. Soc. Am. 67, 393-404.

Peterson, J., H. M. Butler, L. G. Holcomb, and C. R. Hutt (1976). The Seismic Research Observatory, Bull. Seism. Soc. Am. 66, 2049-2068.

Peterson, J., C. R. Hutt, and L. G. Holcomb (1980). Test and calibration of the Seismic Research Observatory, U. S. Geol. Surv., Open-File Rept. 80-187.

Satô, Y. (1955). Analysis of dispersed surface waves by means of Fourier Transform, 1, Bull. Earthquake Inst., Tokyo Univ., 33, 33-48.

Seneff, S. (1978). A fast new method for frequency-filter analysis of surface waves: application in the West Pacific, Bull. Seism. Soc. Am. 68, 1031-1048.

FIGURE CAPTIONS

Figure 1. The 'averaging regions' of several α values in the velocity-log period plane at an epicentral distance of 9453.61 km.

Figure 2. Seismograms used for various numerical tests. The top trace is an observed long-period SRO seismogram. The bottom two traces are synthetic seismograms.

Figure 3. The group velocity dispersion curves of synthetic seismograms A and B.

Figure 4. The amplitude spectra of synthetic seismograms A and B.

Figure 5. Comparison of amplitude spectra of observed seismogram with noise. The smooth curve is the amplitude spectrum of synthetic seismogram B.

Figure 6. The Gaussian parameter α of CRBF, DEF and OBF used to analyze the seismograms shown in Figure 2.

Figure 7. The results of FTAN with CRBF using the observed seismogram in Figure 2.

Figure 8. The results of FTAN with DEF using the observed seismogram in Figure 2.

Figure 9. The results of FTAN with OBF using the observed seismogram in Figure 2.

Figure 10. Systematic errors in group velocity determination using FTAN with CRBF and OBF to analyze synthetic seismogram A.

Figure 11. Systematic errors in amplitude estimate using FTAN with CRBF and OBF to analyze synthetic seismogram A.

Figure 12. The measurement procedure of the 'matched-filter FTAN' technique.

Figure 13. Systematic errors in group velocity using MF-FTAN (first iteration) to analyze synthetic seismograms A and B.

Figure 14. Systematic errors in amplitude using MF-FTAN (first iteration) to analyze synthetic seismograms A and B.

Figure 15. Systematic errors in amplitude using MF-FTAN (second iteration) to analyze synthetic seismogram A.

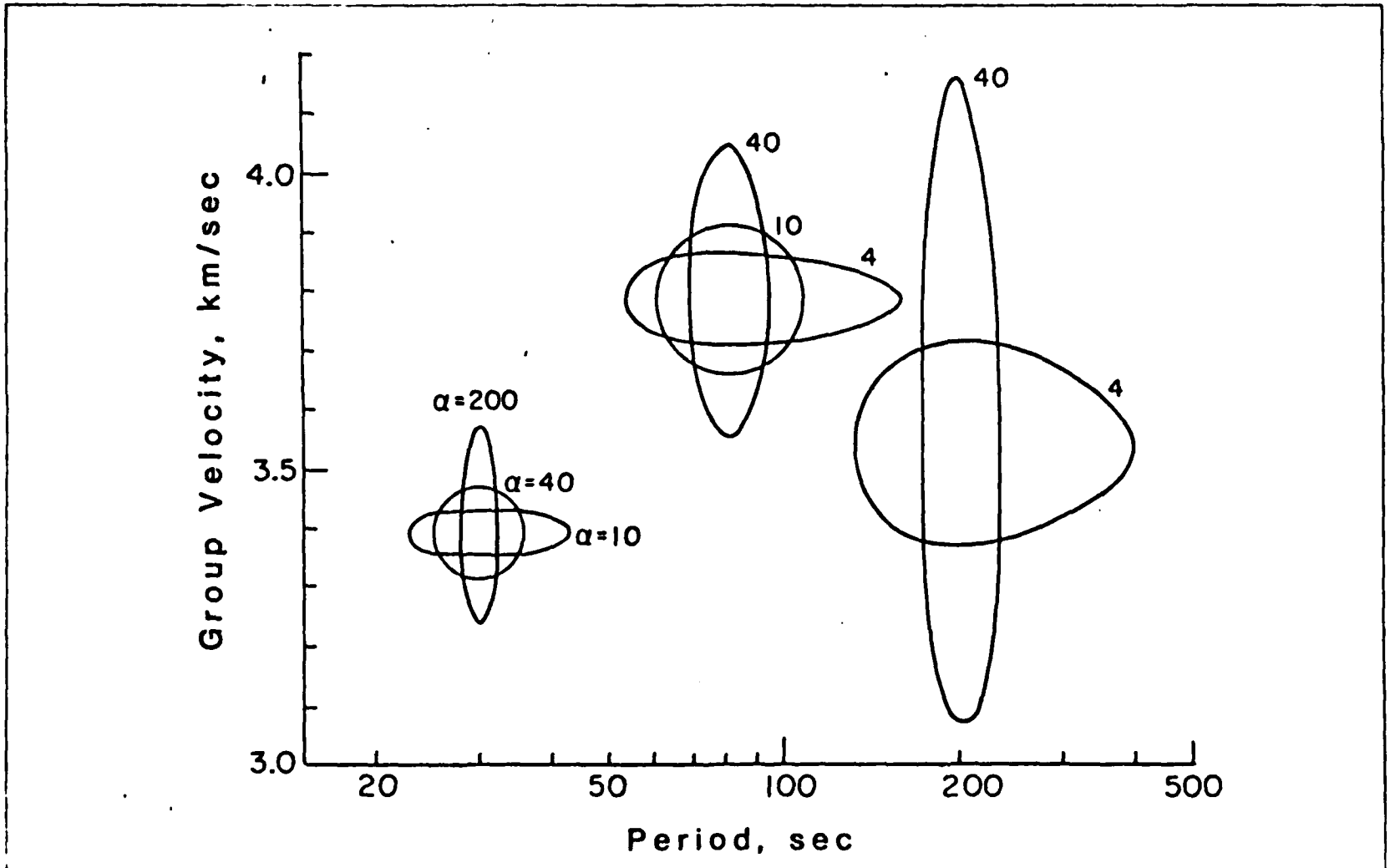
Group Velocity, km/sec
4.0
3.5
3.0
20
50
100
200
500
Period, sec
α=200
α=40
α=10
40
10
4
40
4

Figure 1.

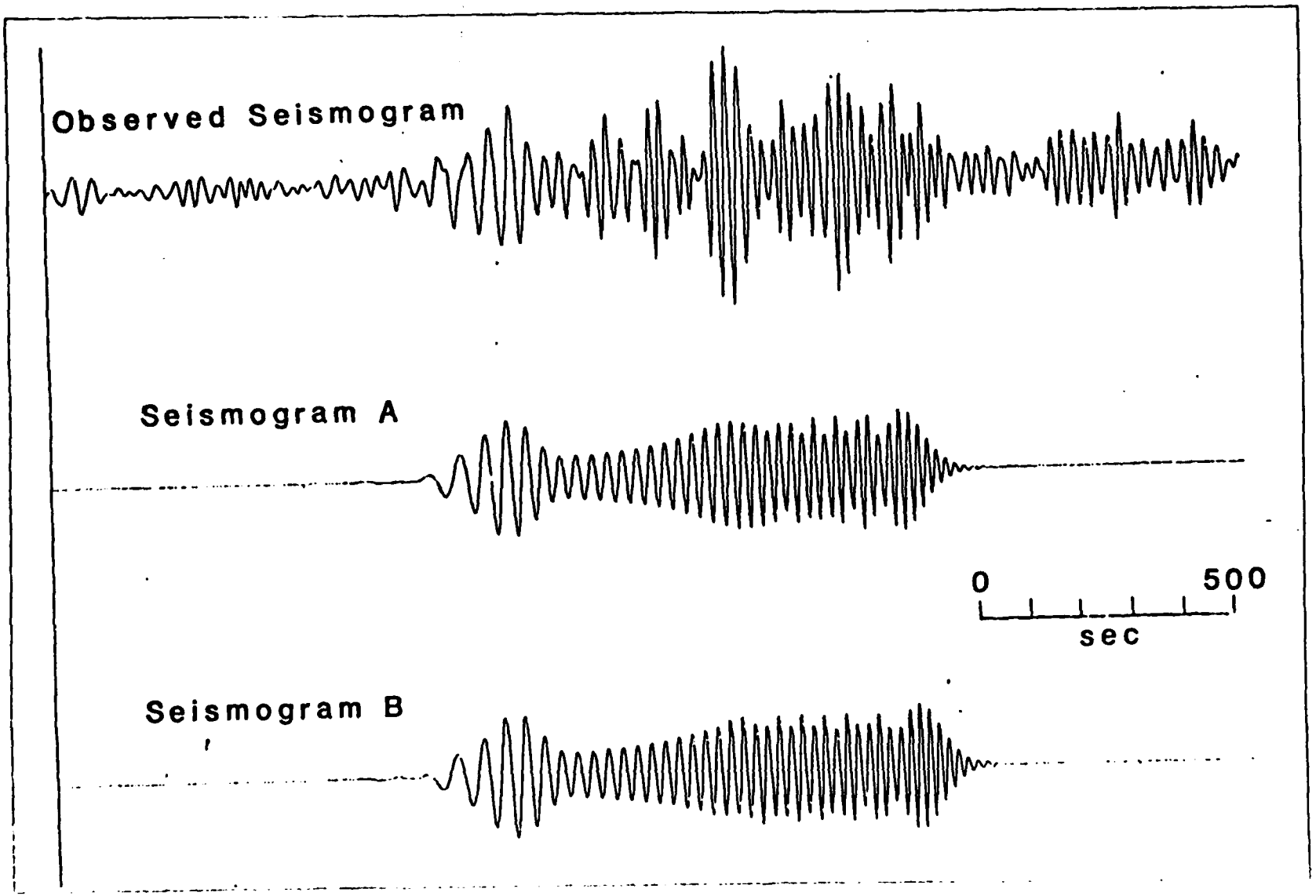

Figure 2.

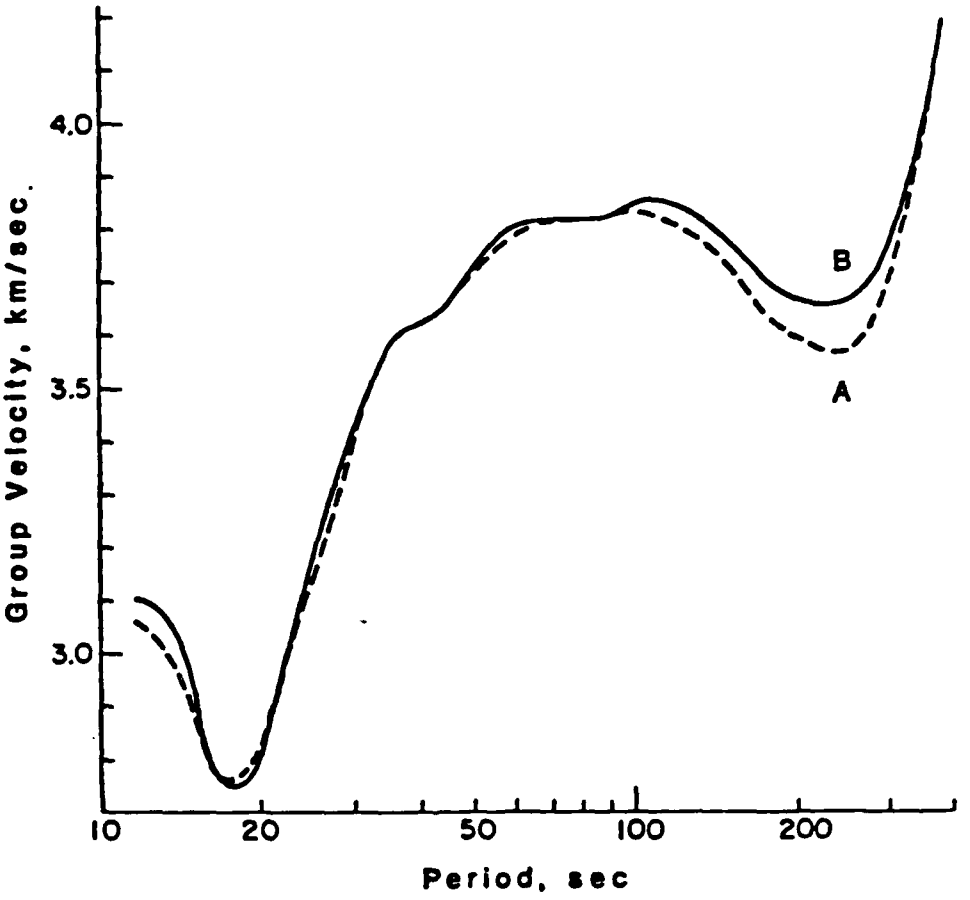

Figure 3.

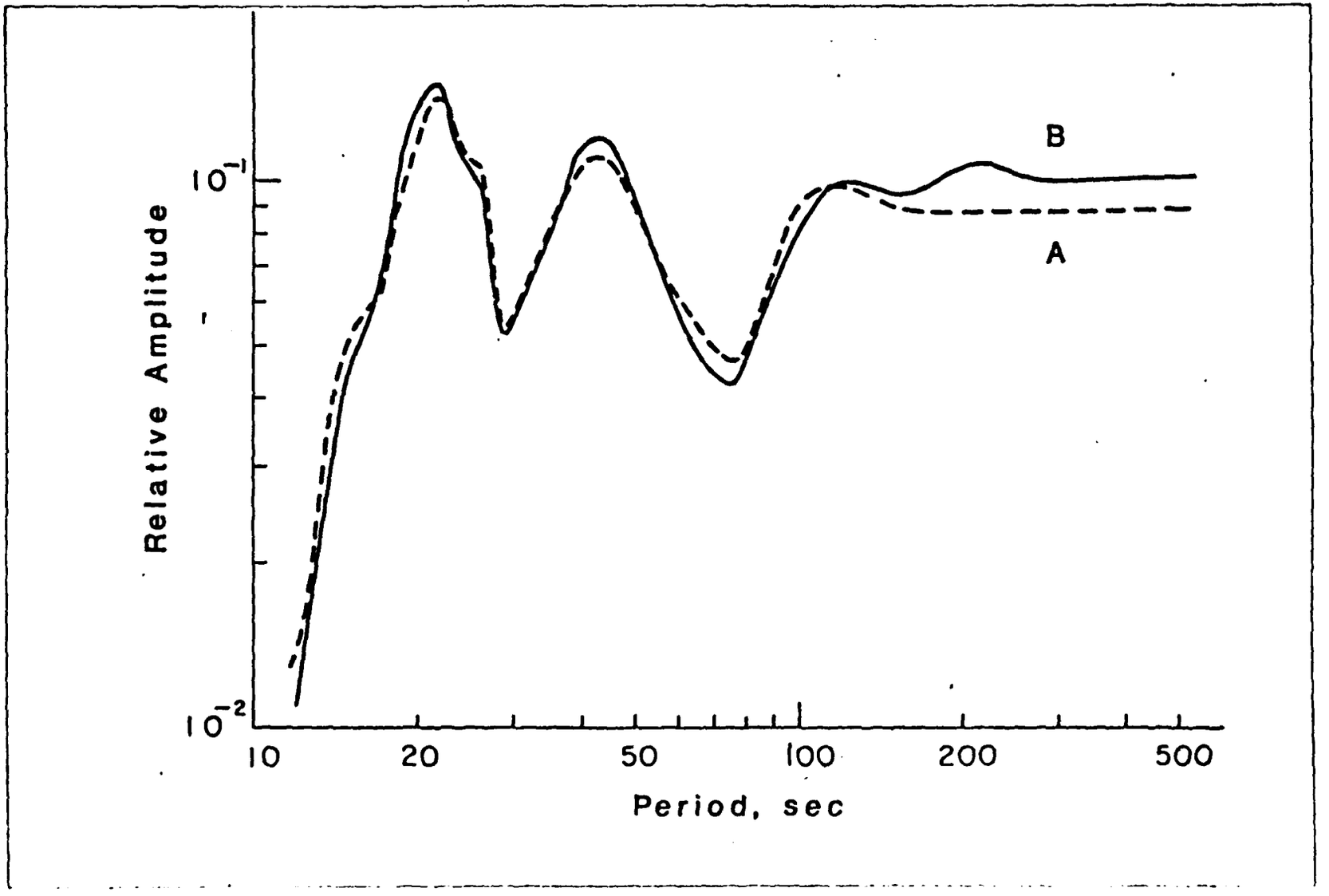

Figure 4.

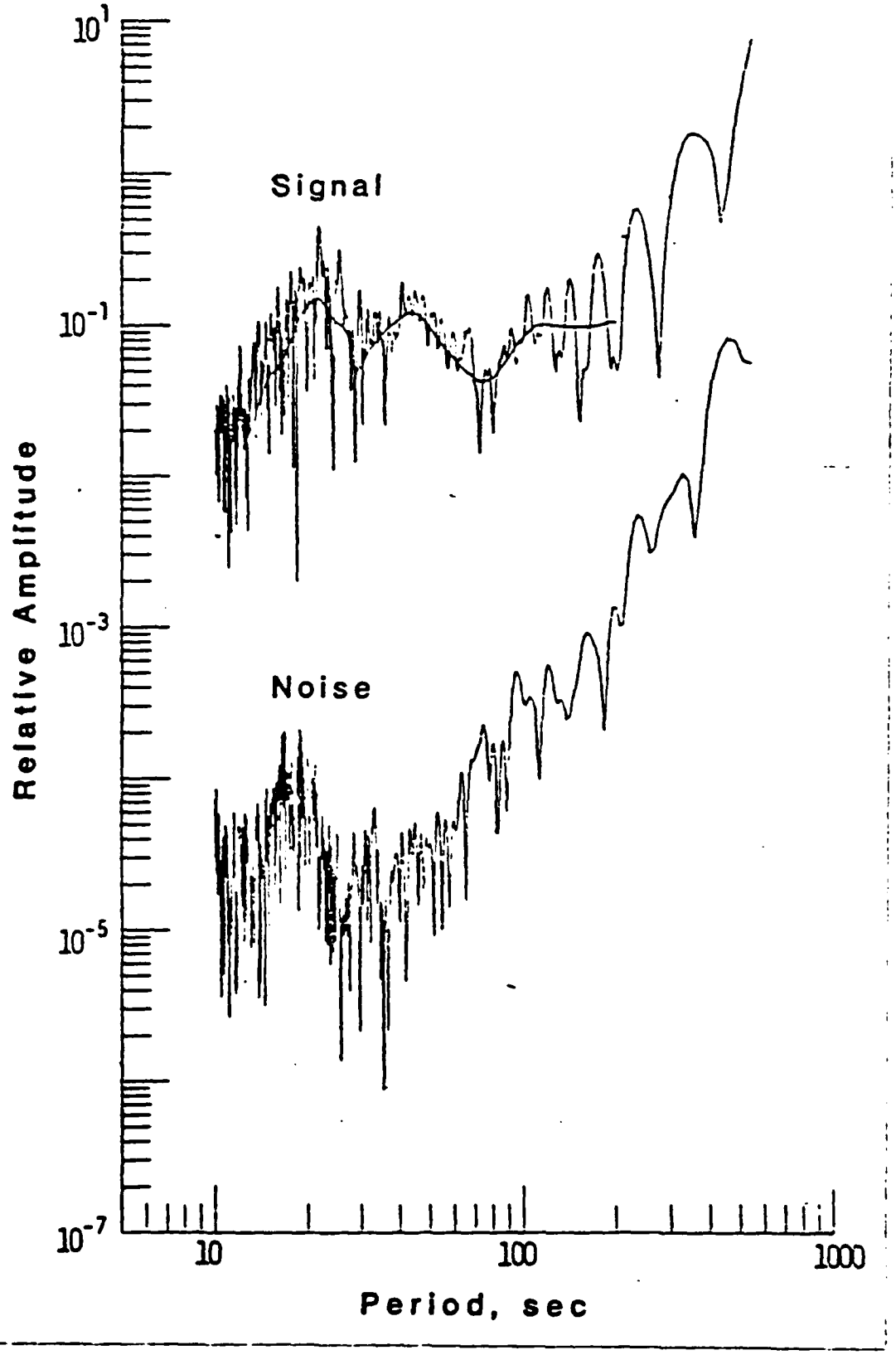
Signal
Noise
Relative Amplitude
10^{1}
10^{-1}
10^{-3}
10^{-5}
10^{-7}
10
100
1000
Period, sec

Figure 5.

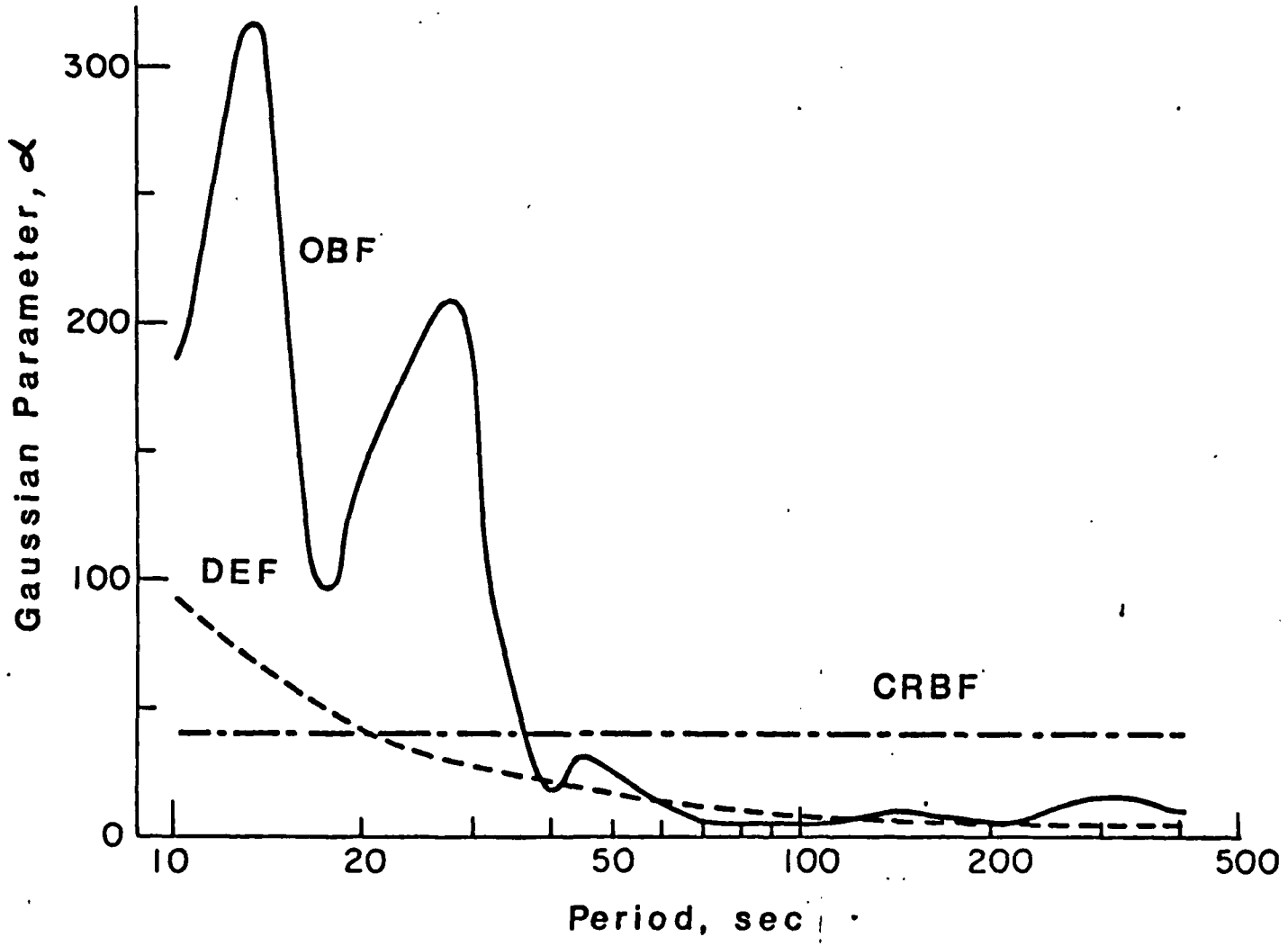
300
200
100
0
Gaussian Parameter, α
OBF
DEF
CRBF
10
20
50
100
200
500
Period, sec

Figure 6.

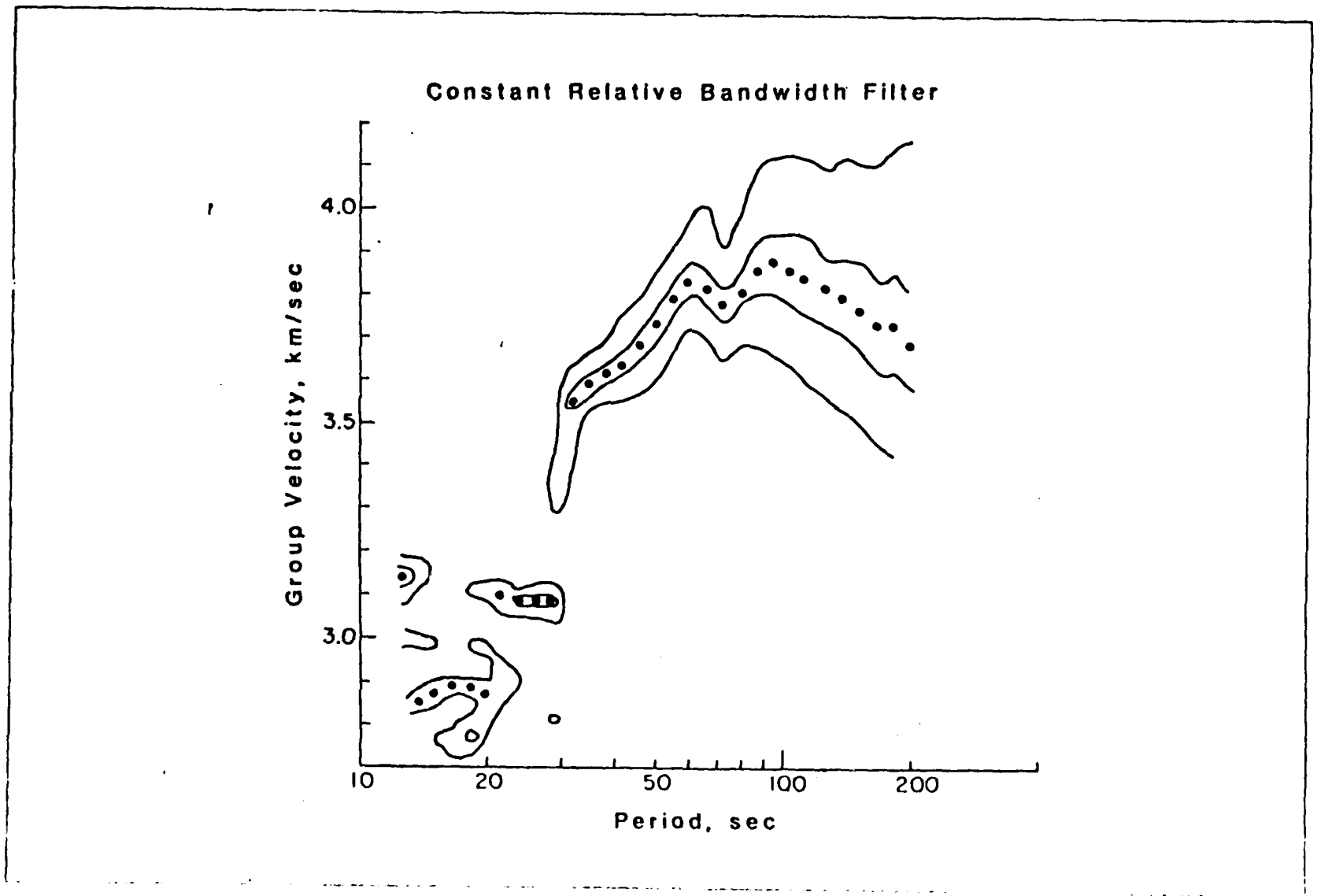
Constant Relative Bandwidth Filter
Group Velocity, km/sec
4.0
3.5
3.0
10
20
50
100
200
Period, sec

Figure 7.

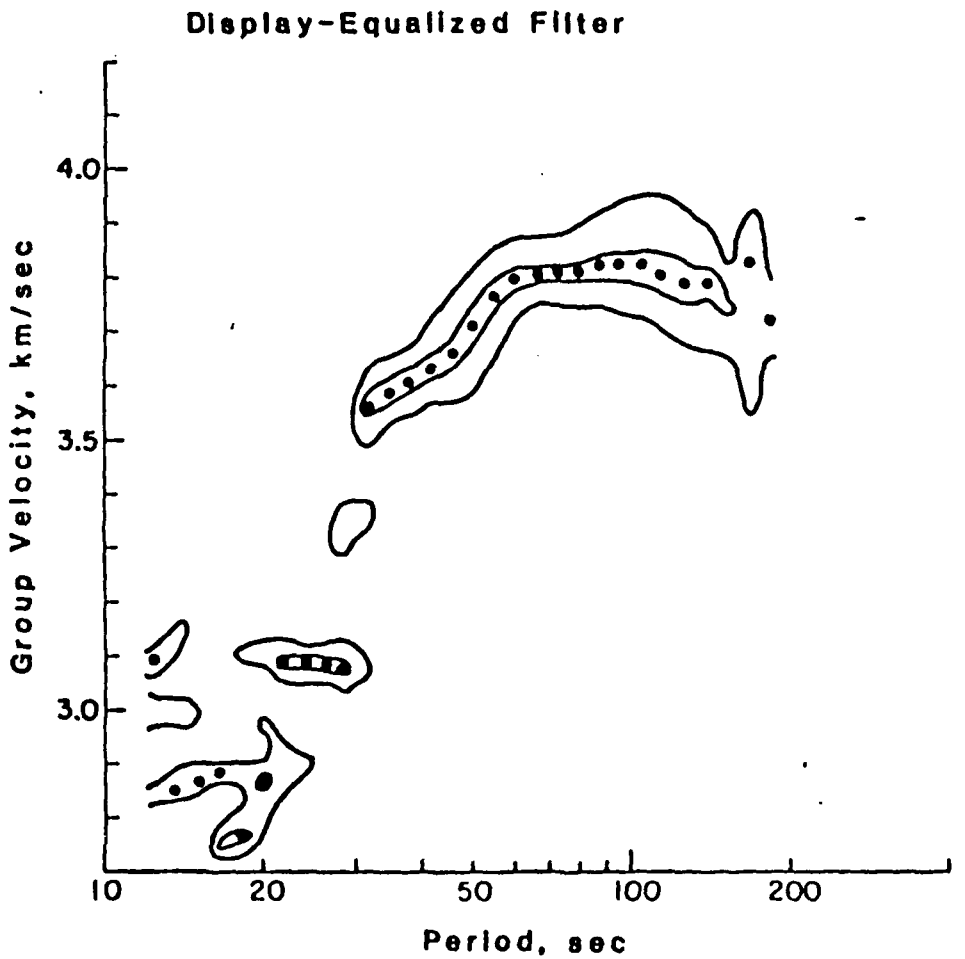
Display-Equalized Filter
Group Velocity, km/sec
4.0
3.5
3.0
10
20
50
100
200
Period, sec

Figure 8.

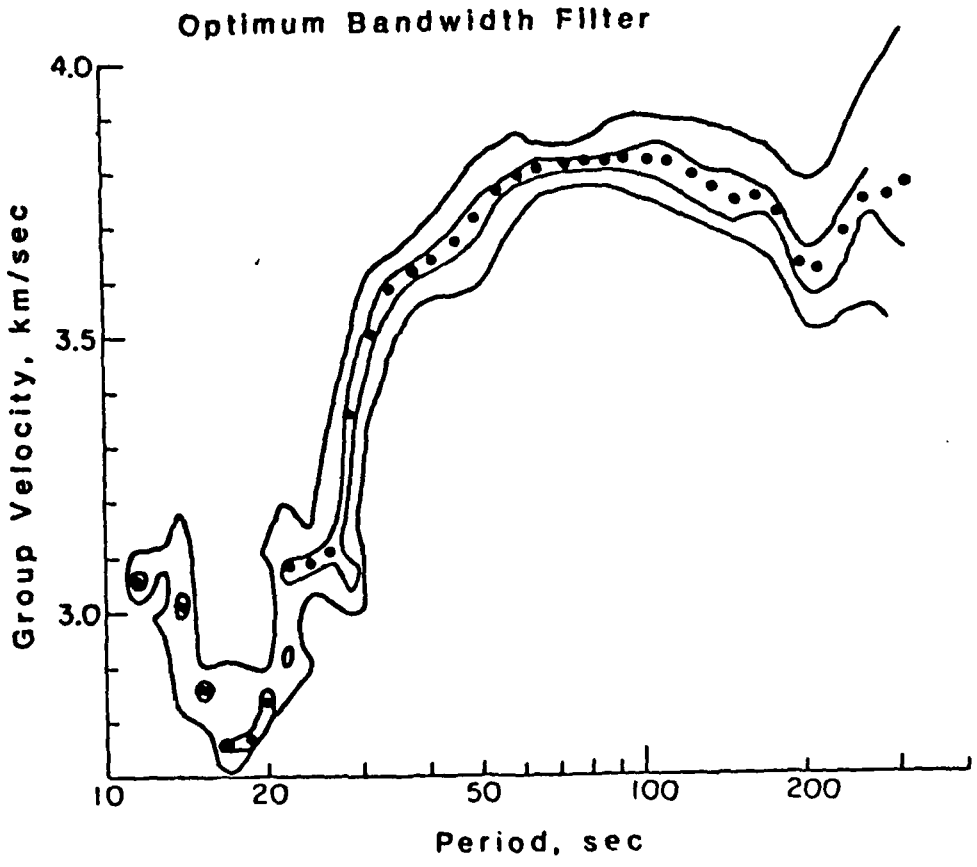
Optimum Bandwidth Filter
4.0
3.5
3.0
Group Velocity, km/sec
10
20
50
100
200
Period, sec

Figure 9.

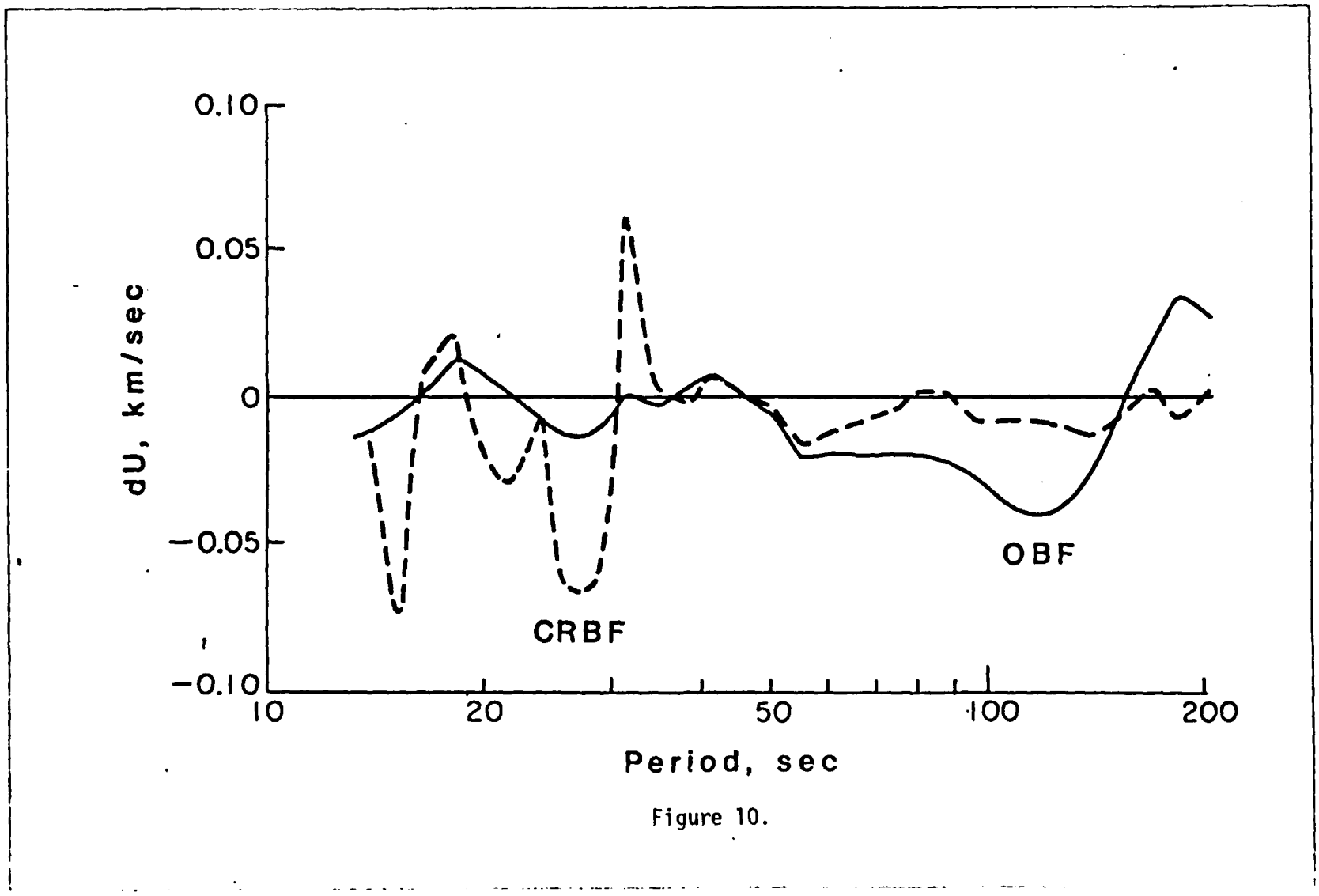

Figure 10.

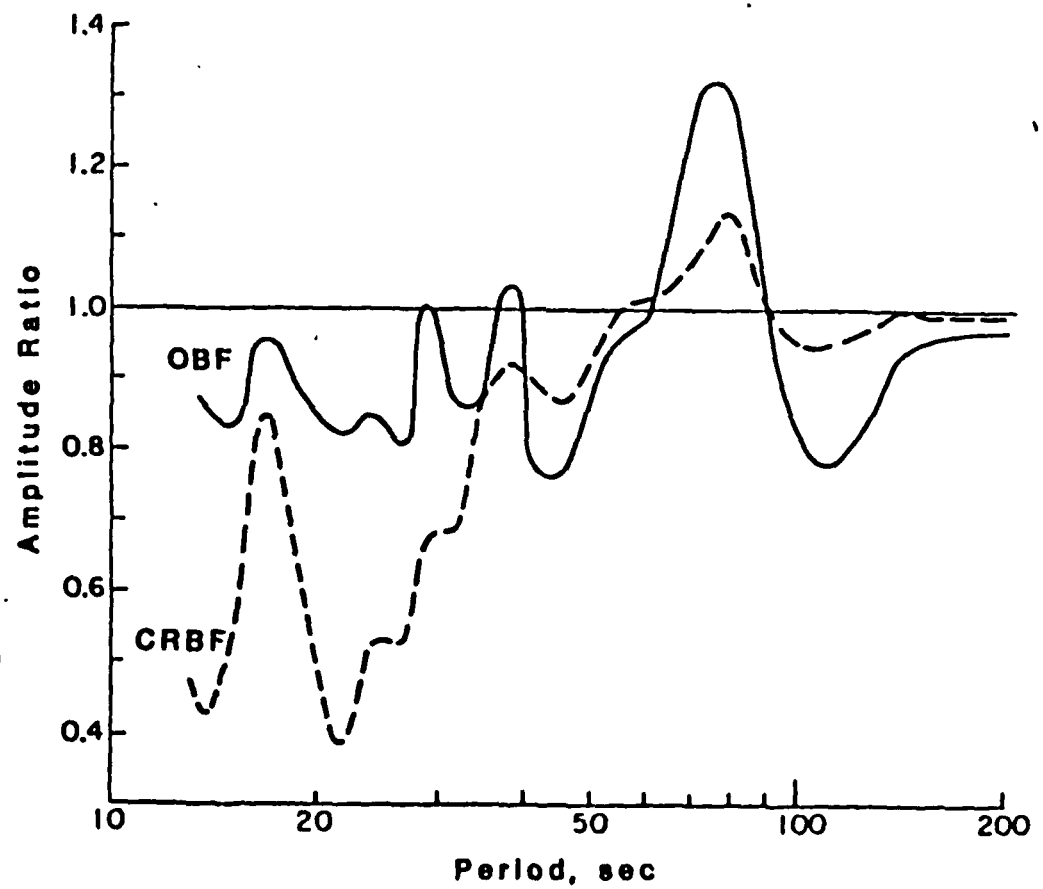
1.4
1.2
1.0
0.8
0.6
0.4
Amplitude Ratio
OBF
CRBF
10
20
50
100
200
Period, sec

Figure 11.

Measurement Procedure

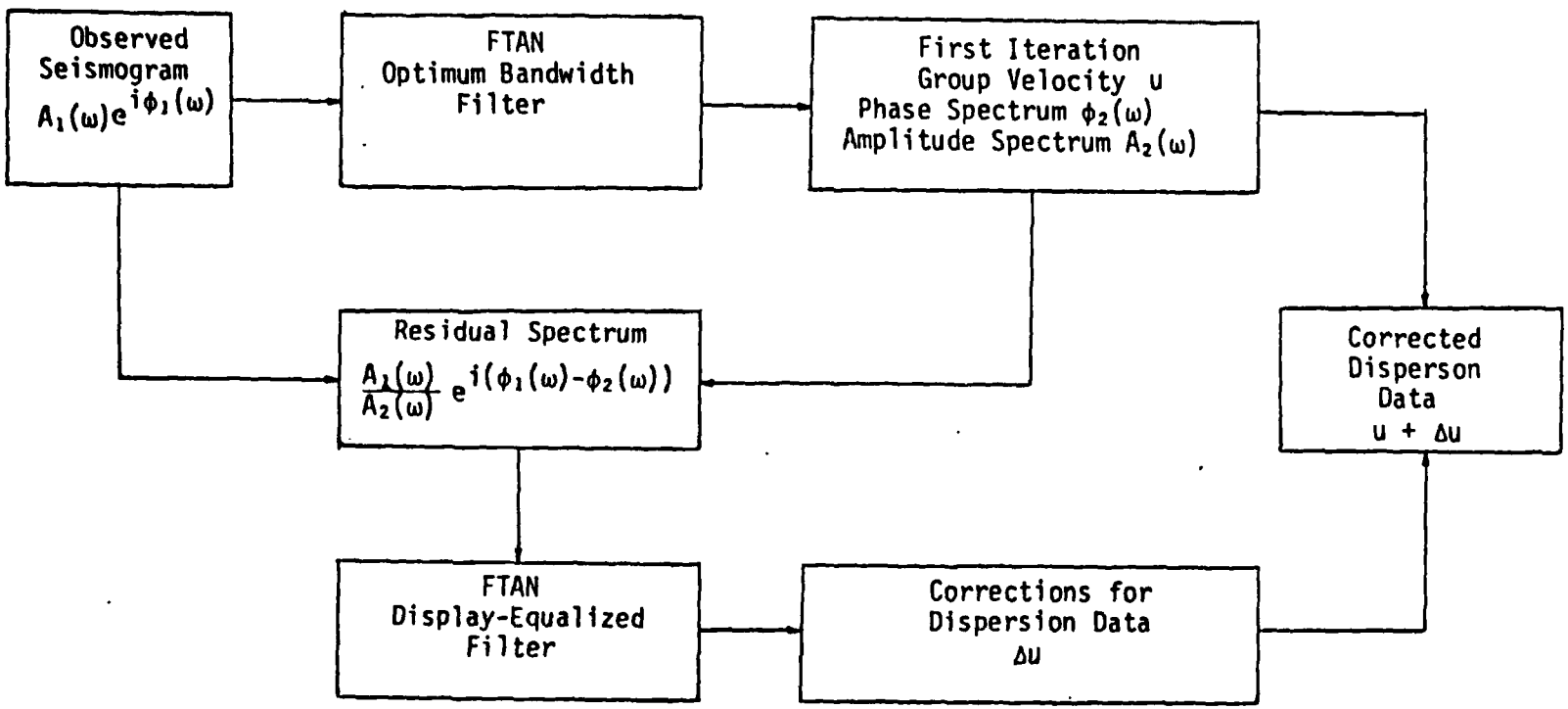

Figure 12.

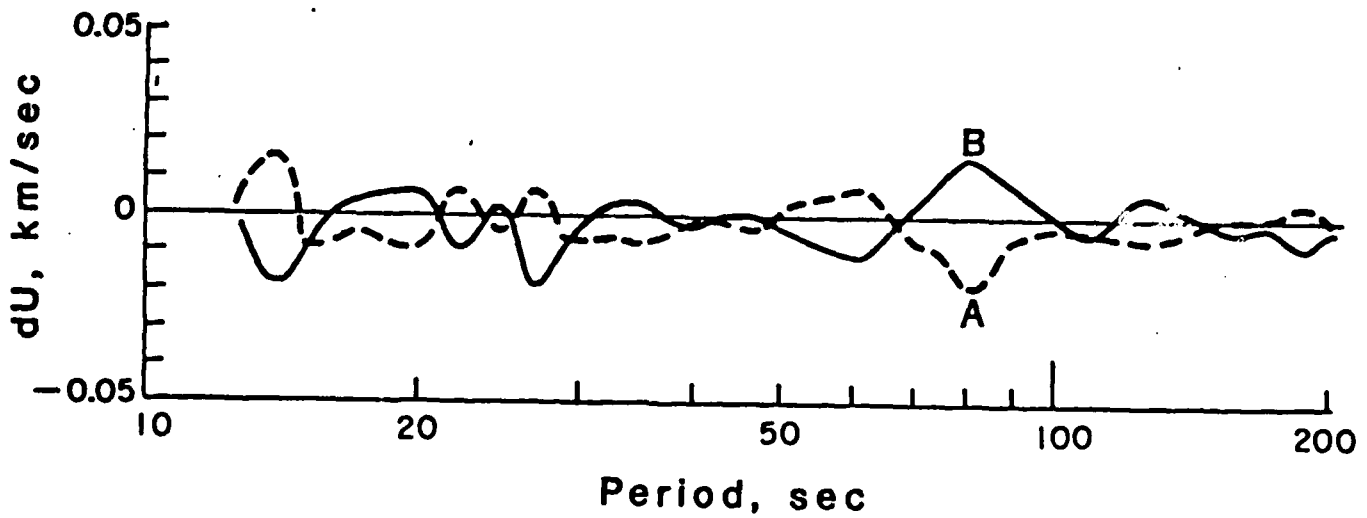

Figure 13.

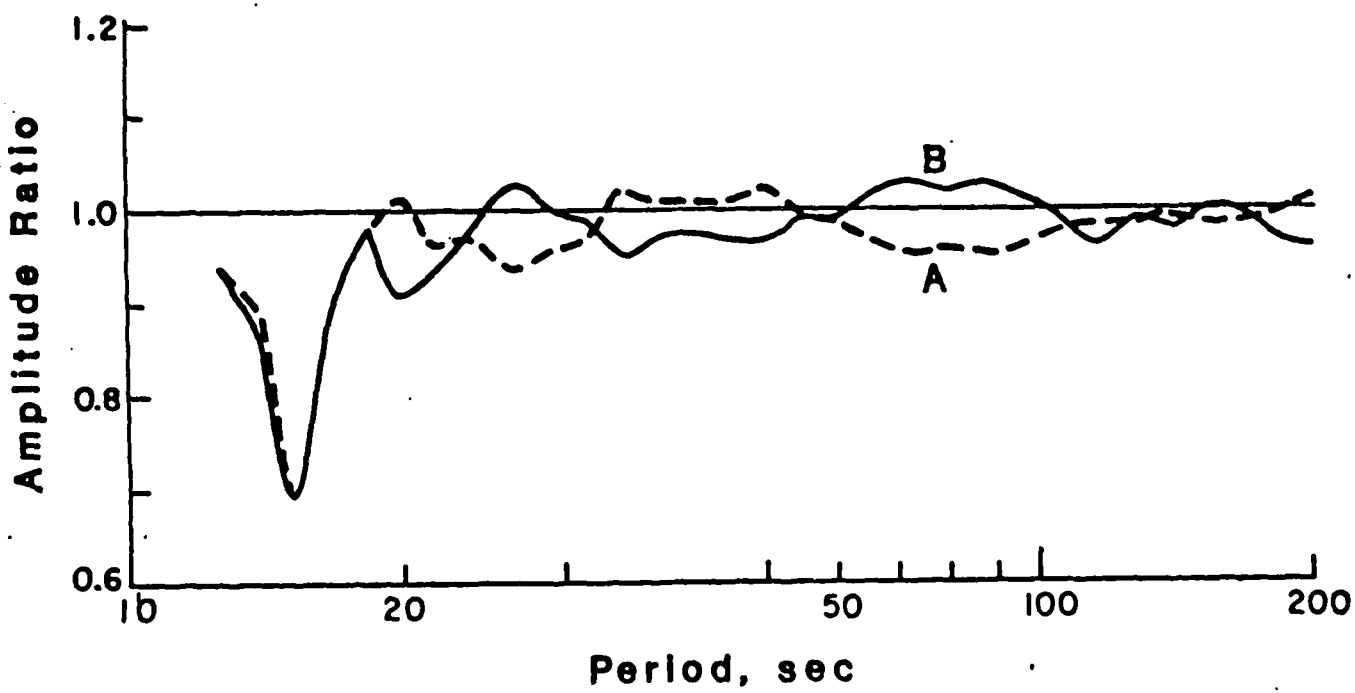

Figure 14.

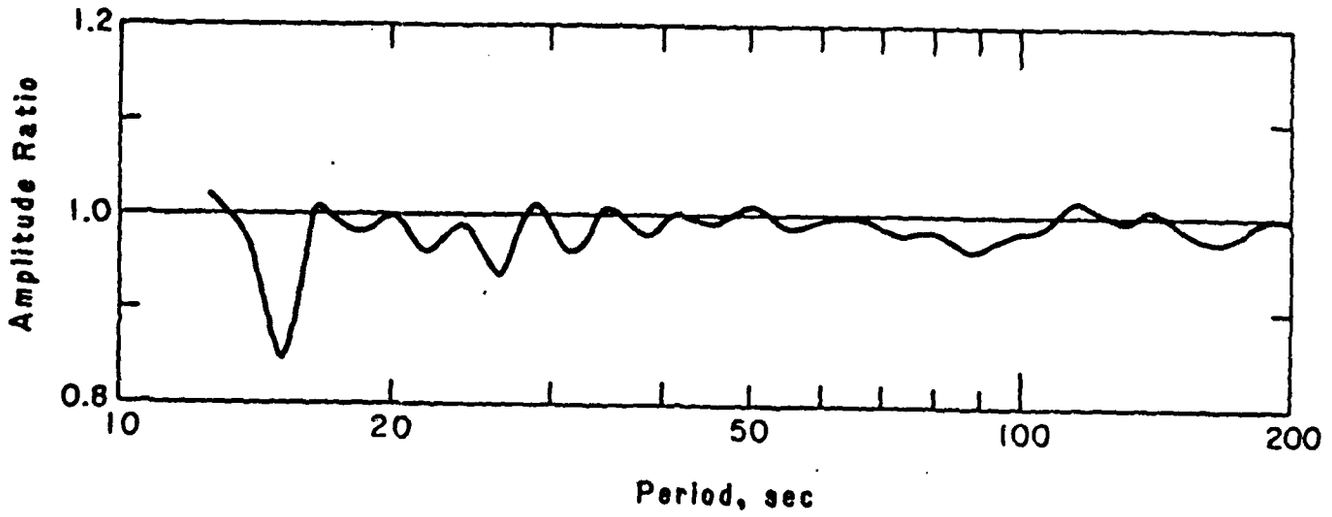

Figure 15.